GeroScience (2017) 39:33–42
DOI 10.1007/s11357-017-9964-z

ORIGINAL ARTICLE

Cerebromicrovascular dysfunction predicts cognitive decline and gait abnormalities in a mouse model of whole brain irradiation-induced accelerated brain senescence

Zoltan Ungvari · Stefano Tarantini · Peter Hertelendy · M. Noa Valcarcel-Ares · Gabor A. Fülöp · Sreemathi Logan · Tamas Kiss · Eszter Farkas · Anna Csiszar · Andriy Yabluchanskiy

Received: 10 January 2017 / Accepted: 25 January 2017 / Published online: 4 February 2017

Abstract Whole brain irradiation (WBI) is a mainstream therapy for patients with both identifiable brain metastases and prophylaxis for microscopic malignancies. However, it also promotes accelerated senescence in healthy tissues and leads to progressive cognitive dysfunction in up to 50% of tumor patients surviving long term after treatment, due to γ-irradiation-induced cerebromicrovascular injury. Moment-to-moment adjustment of cerebral blood flow (CBF) via neuronal activity-dependent cerebromicrovascular dilation (functional hyperemia) has a critical role in maintenance of healthy cognitive function. To determine whether cognitive decline induced by WBI associates with impaired cerebromicrovascular function, C56BL/6 mice (3 months) subjected to a clinically relevant protocol of fractionated WBI (5 Gy twice weekly for 4 weeks) and control mice were compared. Mice were tested for spatial memory performance (radial arm water maze), sensorimotor coordination (computerized gait analysis, CatWalk), and cerebromicrovascular function (whisker-stimulation-induced increases in CBF, measured by laser Doppler flowmetry) at 3 to 6 months post-irradiation. We found that mice with WBI exhibited impaired cerebromicrovascular function at 3 months post-irradiation, which was associated with impaired performance in the radial arm water maze. At 6 months, post-irradiation progressive impairment in gait coordination (including changes in the regularity index and phase dispersion) was also evident. Collectively, our findings provide evidence for early and persisting neurovascular impairment after a clinically relevant protocol of fractionated WBI, which predict early manifestations of cognitive impairment.

Keywords Whole brain irradiation · Neurovascular coupling · Functional hyperemia · Dementia · Gait dysfunction · Neurovascular unit · Cellular senescence · DNA damage

Zoltan Ungvari, Stefano Tarantini, and Peter Hertelendy contributed equally to this work.

Z. Ungvari · S. Tarantini · P. Hertelendy · M. N. Valcarcel-Ares · G. A. Fülöp · S. Logan · T. Kiss · A. Csiszar · A. Yabluchanskiy (✉)
Reynolds Oklahoma Center on Aging, Department of Geriatric Medicine, University of Oklahoma Health Sciences Center, 975 NE 10th Street, BRC 1311, Oklahoma City, OK 73104, USA
e-mail: Andriy-Yabluchanskiy@ouhsc.edu

Z. Ungvari · S. Tarantini · M. N. Valcarcel-Ares · G. A. Fülöp · T. Kiss · E. Farkas · A. Csiszar · A. Yabluchanskiy
Translational Geroscience Laboratory, Donald W. Reynolds Department of Geriatric Medicine, University of Oklahoma Health Sciences Center, Oklahoma City, OK, USA

Z. Ungvari · P. Hertelendy · E. Farkas · A. Csiszar
Department of Medical Physics and Informatics, Faculty of Medicine and Faculty of Science and Informatics, University of Szeged, Szeged, Hungary

Introduction

Whole brain irradiation (WBI) is an important therapeutic treatment in patients with both identifiable brain metastases and prophylaxis for microscopic malignancies (Gaspar et al. 2010; Patil et al. 2012). Over 200,000 tumor patients with brain involvement are treated with

either partial large field or WBI every year in the USA (Lee et al. 2012). Although WBI is clinically effective in eliminating tumor cells, it also results in a range of unwanted side-effects in healthy tissues. In particular, irradiation-induced DNA damage is known to lead to accelerated brain senescence, which promotes functional impairment in the cortex, hippocampus, and white matter months to years after treatment (Khuntia et al. 2006; Welzel et al. 2008a, 2008b). As a result, up to 50% of patients who survive long term after treatment experience progressive dementia, thus severely compromising quality of life (Lee et al. 2012). The available experimental data clearly demonstrate that radiation also leads to a progressive impairment of cognitive function in animal models, mimicking the clinical scenario of cognitive decline in patients after WBI (Lamproglou et al. 2001; Shi et al. 2006; Soussain et al. 2009; Warrington et al. 2012; Welzel et al. 2008a, 2008b). Recent studies show that in addition to its profound harmful effects on cognitive function, WBI can also result in the impairment of other brain functions such as coordination of gait (Hatcher-Martin and Factor 2016). At present, no effective strategies exist to prevent radiation-induced decline in higher brain functions and there are no treatments available to reverse these effects.

Although the mechanisms underlying cognitive deficits after WBI are likely multifaceted, there is increasing pre-clinical and clinical evidence that WBI compromises the structural integrity of the cerebral microcirculation, which significantly contributes to cognitive impairment (Ashpole et al. 2014; Warrington et al. 2011, 2012, 2013). Previous studies demonstrate that clinical series of fractionated WBI induce a 40% decrease in capillary density in the brain regions associated with learning and memory (Warrington et al. 2012), mimicking aging phenotype. Despite these advances, there are no studies available elucidating the functional consequences of WBI-induced accelerated brain senescence on the cerebral microvasculature. Normal brain function is critically dependent on a continuous, tightly controlled supply of oxygen and glucose through cerebral blood flow (CBF). Although energetic demands of neurons are very high, the brain has very little reserve capacity. During periods of intense neuronal activity, there is a requirement for rapid increases in oxygen and glucose delivery. This is ensured by neurovascular coupling (functional hyperemia), a vital mechanism of regulation of CBF that maintains optimal microenvironment of cerebral tissue by adjusting local blood flow to local neuronal activity in a moment-to-moment manner (Attwell et al. 2010; Tarantini et al. 2015, 2016; Toth et al. 2016; Toth et al. 2014a, 2015a, 2015b, 2017; Tucsek et al. 2014). There is increasing evidence that neurovascular dysfunction is causally related to cognitive decline in models of aging (Tarantini et al. 2015, 2016), yet, the effects of WBI on cerebromicrovascular function have never been investigated.

The present study was designed to test the hypothesis that WBI-induced accelerated brain senescence associates with early-onset cerebromicrovascular dysfunction. To achieve this goal, C56BL/6 mice were subjected to a clinically relevant protocol of fractionated WBI (5 Gy twice weekly for 4 weeks). WBI-treated and control mice were tested for spatial memory performance (radial arm water maze), sensorimotor coordination (computerized gait analysis, CatWalk), and cerebromicrovascular function (whisker-stimulation-induced increases in CBF, measured by laser Doppler flowmetry) at 3 and 6 months post-irradiation.

Materials and methods

Experimental animals and experimental design

C57BL/6J (3 months old, $n = 51$) mice were purchased from the Jackson Laboratories (Bar Harbor, ME) and housed three per cage in the specific pathogen-free animal facility at the University of Oklahoma Health Sciences Center (OUHSC). Animals were kept on a 12-h light/dark cycle and fed standard rodent chow and water ad libitum. One week before radiation treatment, mice were transferred to the conventional facility (OUHSC) and housed under similar conditions. Mice were anesthetized and subjected to clinical series of WBI ($n = 31$, 5 Gy twice weekly for a total cumulative dose of 40 Gy) or used as a control group ($n = 20$). Mice were left to recover for 3 or 6 months in the original environment. At the end of the recovery period, mice were experimentally tested for cognitive function, gait coordination, and neurovascular coupling responses. All animal protocols were approved by the Institutional Animal Care and Use Committee of OUHSC.

Fractionated whole brain irradiation protocol

After acclimating to the conventional facility for 1 week, mice were randomly assigned to either anesthetized

control or radiated groups. Animals were weighed and anesthetized via intra-peritoneal injection of ketamine and xylazine (100/15 mg per kg). Mice in the radiated group were subjected to clinical series of WBI (5 Gy twice weekly for a total cumulative dose of 40 Gy). Radiation was administered using a ^{137}Cesium gamma irradiator (GammaCell 40, Nordion International). A Cerrobend® shield was utilized to minimize the dose to the bodies of mice in the radiated group. The radiation dose received by the mice was verified using film dosimetry, as described (Warrington et al. 2011, 2012).

Radial arms water maze testing

To determine how accelerated brain senescence induced by WBI affects cognitive function, spatial memory and long-term memory was tested in mice by assessing performance in the radial arms water maze at 3 or 6 months post-WBI treatment. The maze consisted of eight arms with a submerged escape platform located at the end of one of the arms. Food coloring paint was added into the water to make it opaque. The maze was surrounded by privacy blinds with extramaze visual cues. Intramaze visual cues were placed at the end of the arms. The mice were monitored by a video tracking system directly above the maze as they waded and parameters were measured using Ethovision software (Noldus Information Technology Inc., Leesburg, VA, USA). Experimenters were unaware of the experimental conditions of the mice at the time of testing. During the learning period each day, mice were given the opportunity to learn the location of the submerged platform during two session blocks each consisting of four consecutive acquisition trials. On each trial, the mouse was started in one arm not containing the platform and allowed to wade for up to 1 min to find the escape platform. All mice spent 30 s on the platform following each trial before beginning the next trial. The platform was located in the same arm on each trial. Over 3 days of training, mice gradually improved performance as they learned the procedural aspects of the task. Upon entering an incorrect arm (all four paws within the distal half of the arm), the mouse was charged an error. Learning capability was assessed by comparing performance on days 2 and 3 of the learning period. When eventually both groups learned the procedural aspects of the task, the mice were placed in their home cage for 7 days. Then, the mice were administered the recall trial on day 10. On day 11 (extinction), mice were tested for ability to relearn the task, when the platform has been moved to a different arm which was not adjacent nor diametrically positioned to the previous location. Mice were tested for two session blocks and the second block consisting of four trials has been used for comparison.

Analysis of gait function

To determine how accelerated brain senescence induced by WBI affects gait coordination, we tested the animals using an automated computer assisted method (CatWalk; Noldus Information Technology Inc.) at 3 and 6 month post-WBI. Using the CatWalk system, the detection of paw print size and paw placement patterns during volunteer running on an illuminated glass walkway by a camera placed under the glass surface provides an automated analysis of gait function and the spatial and temporal aspects of inter-limb coordination (Tarantini et al. 2015). Briefly, animals were trained to cross the walkway and then, in a dark and silent room (<20 lx of illumination), animals were tested in three consecutive runs. Data were averaged across ten runs in which the animal maintained a constant speed across the walkway.

The variability of the data has been assessed using quartile dispersion. We adopted a common outlier definition, labeling points more than 1.5 interquartile ranges away from the sample median as extreme values. After variability analyses, the following indices were calculated. The regularity index (%) is a fractional measure of interpaw coordination, which expresses the number of normal step sequence patterns relative to the total number of paw placements. The formula of regularity index is NSSP × 4/PP × 100 (%), where NSSP represents the number of normal step sequence patterns and PP the total number of paw placements. In healthy, fully coordinated animals, its value is close to 100%. Phase dispersion provides a quantitative metric of interpaw coordination. Phase dispersion characterizes the placement of two paws ("target" and "anchor") during the cycle of consecutive initial contacts with an "anchor" paw. In a step cycle, base of support gives the distance between the mass midpoints of the fore prints at maximal contact. The results are averaged and expressed in centimeters.

Assessment of neurovascular coupling responses

To determine how accelerated brain senescence induced by WBI affects cerebromicrovascular function, cerebral blood flow responses to whisker stimulation were

assessed at 3 months post-WBI treatment. Mice were anesthetized (α-chloralose, 50 mg/kg plus urethane, 750 mg/kg, i.p.), endotracheally intubated and ventilated (MousVent G500; Kent Scientific Co, Torrington, CT). Rectal temperature was maintained at 37 °C using a thermostatic heating pad (Kent Scientific Co, Torrington, CT). End-tidal CO_2 (with dead space) was kept between 3.2 and 3.7% to maintain blood gas values within the physiological range, as reported (Toth et al. 2014a). Animals were immobilized and placed on a stereotaxic frame (Leica Microsystems Inc., Buffalo Grove, IL). The scalp and periosteum were pulled aside and a craniotomy was made with a dental drill over the left somatosensory cortex corresponding to the barrel field as described (Toth et al. 2015b). The dura was gently removed, and the open cranial window was continuously superfused with artificial cerebrospinal fluid (ACSF, composition: NaCl 119 mM, $NaHCO_3$ 26.2 mM, KCl 2.5 mM, NaH_2PO_4 1 mM, $MgCl_2$ 1.3 mM, glucose 10 mM, $CaCl_2$ 2.5 mM, pH = 7.3, 37 °C). The right femoral artery was cannulated for arterial blood pressure measurement (Living Systems Instrumentations, Burlington, VT) to ensure that the blood pressure was within the physiological range throughout the experiments (90–100 mmHg). To assess neurovascular coupling, a laser Doppler probe (Transonic Systems Inc., Ithaca, NY) was positioned above the barrel cortex (1–1.5 mm posterior and 3–3.5 mm lateral to bregma), and the contralateral whiskers were stimulated for 30 s at 5 Hz from side to side, as previously described (Toth et al. 2014a, 2015b). Changes in CBF (n = 7–8 in each group) were assessed in three trials divided by 5–10 min intervals and are expressed as percent (%) changes from baseline.

WBI could affect functional hyperemia by impairing neural activity evoked by whisker stimulation. To examine this possibility, we recorded spontaneous and evoked neural activity in control and WBI-treated mice. A glass-insulated tungsten microelectrode (impedance, 2–3 MΩ; Kation Scientific, LLC, Minneapolis, MN, USA) was inserted into the left barrel cortex (1–1.5 mm posterior and 3–3.5 mm lateral to bregma) through the ACSF-perfused open cranial window for recording local field potentials as described (Toth et al. 2015a). An Ag/AgCl electrode inserted in the neck muscles served as reference. After basal activity was recorded, the right whisker pad was stimulated by a bipolar-stimulating electrode placed to the ramus infraorbitalis of the trigeminal nerve and into the masticatory muscles. The stimulation protocol used to investigate neurovascular coupling and somatosensory evoked field potentials consisted of ten stimulation presentation trials with an intertrial interval of 70 s, each delivering a 15-s train of electrical pulses (2 Hz, 0.2 mA, intensity, and 0.3 ms pulse width) after a 10-s prestimulation baseline period. The signal was amplified with an AC/DC differential amplifier (high pass at 1 Hz, low pass at 1 kHz) (Model 3000; A-M Systems, Inc. Carlsborg, WA, USA) and digitalized by the PowerLab/Labchart data acquisition system (ADInstruments, Colorado Springs, CO, USA) with a sampling rate of 40 kHz. Basal activity was analyzed as distribution of wave amplitude as a function of frequency, and the negative amplitude in the somatosensory evoked field potential response was considered as the excitatory postsynaptic potential (Toth et al. 2014b). Analyses were performed on the average of ten stimulation trials.

Statistical analysis

Statistical analysis was carried out by unpaired t test, one-way ANOVA, or two-way ANOVA for repeated measures followed by Bonferroni multiple comparison test, as appropriate, using Prism 5.0 for Windows (Graphpad Software, La Jolla, CA). A p value less than 0.05 was considered statistically significant. Data are expressed as mean ± S.E.M.

Results

Cognitive function is impaired in mice by 3 months post-WBI

Previously, we demonstrated that C57BL/6J mice exhibit significant impairment of hippocampal-encoded functions of learning and memory at 5 months post-WBI treatment (Warrington et al. 2013). To gain insight into the time-course of the development of irradiation-induced cognitive decline, in the present study, we assessed learning and memory function in mice 3 months post-WBI and in age-matched controls in the radial arm water maze (Fig. 1a, left and right panel, respectively). We compared the learning performance of mice in each experimental group by analyzing the day-to-day changes in the path length and error rate. The error rate is the sum of all incorrect arm entries, where

each error corresponds to each incorrect entry. The error rate for each mouse is then averaged among each experimental group in every trial block. During acquisition, mice from all groups showed a decrease in the path length (Fig. 1a) and the combined error rate (Fig. 1b) across days, indicating learning of the task. We found that control mice and mice at 3 months post-WBI exhibited similar learning during the first 3 days of testing (Fig. 1b, c). We confirmed that mice exhibited significant impairment of learning function when tested 6 months post-WBI (data not shown). Memory recall 7 days later was also similar in both groups. WBI-treated mice showed impaired extinction ability on day 11 (Fig. 1b, c). The extinction blocks describe the ability of the mouse to forget and relearn the task with a different platform location. These findings suggest that learning plasticity is impaired early after WBI treatment and precedes impairment in learning and memory. These data are consistent with the progressive development of cognitive impairment post-WBI.

Mild gait dysfunction becomes evident 6 months post-WBI

We performed gait analyses using the Catwalk system in control and WBI-treated animals. We found that WBI-treated mice showed no difference in gait coordination at 3 months post-irradiation (Fig. 2a–f). However, when followed further for another 3 months, significantly lower regularity index and significantly higher phase dispersion was evident in WBI-treated mice as compared to controls (Fig. 3). These data suggest that gait

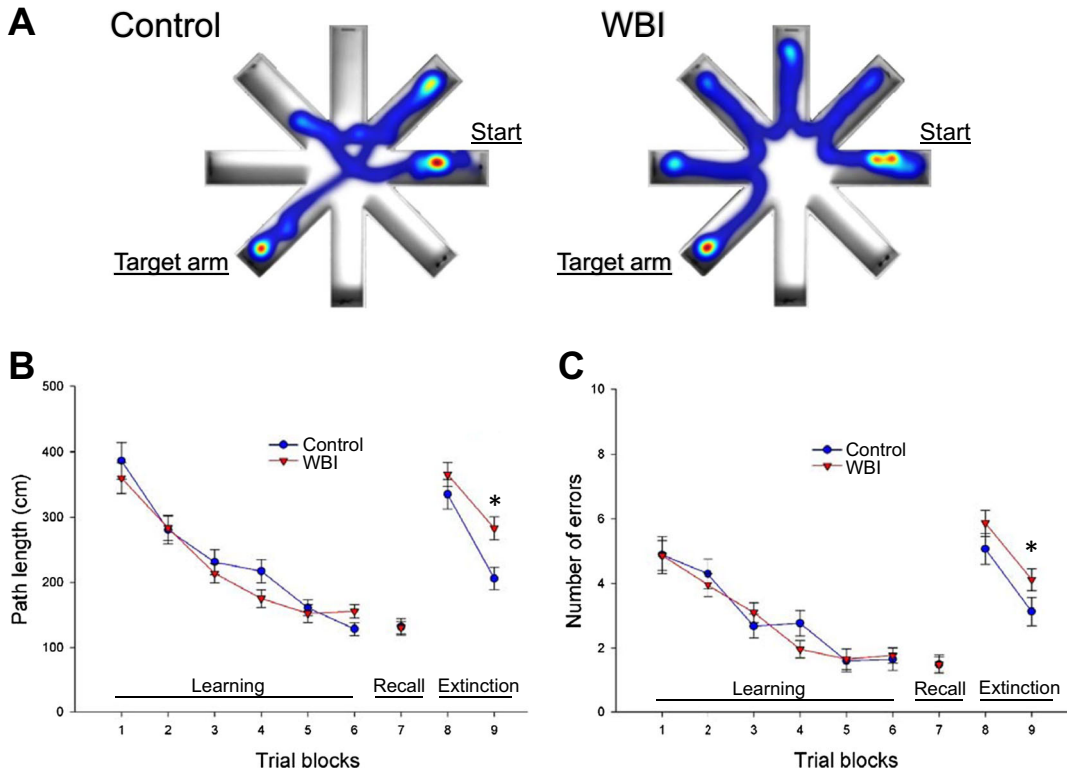

Fig. 1 WBI treatment results in impaired radial arm water maze (RAWM) performance in mice. WBI-treated mice and aged-matched control mice were tested in the RAWM 3 months post-WBI. **a** Heatmaps representing the percentage of time spent in different locations in the maze for a randomly selected control (*left*) and WBI-treated (*right*) animal during experimental day 11 in trial block 9. **b** Average path length required to reach the hidden platform in the RAWM. During acquisition (trial blocks 1 to 6) and memory recall (trial block 7) in WBI-treated mice, the average path length required to reach the hidden platform did not differ from that in control mice at 3 months post-irradiation. Combined error rates (**c**) were also similar in both groups during acquisition (trial blocks 1 to 6) and memory recall (trial block 7). In contrast, WBI-treated animals traveled longer distance (**b**) and made more errors (**c**) before they were able to relearn the task when the platform was moved to a different location during extinction phase. Data are mean ± SEM (*$p < 0.05$)

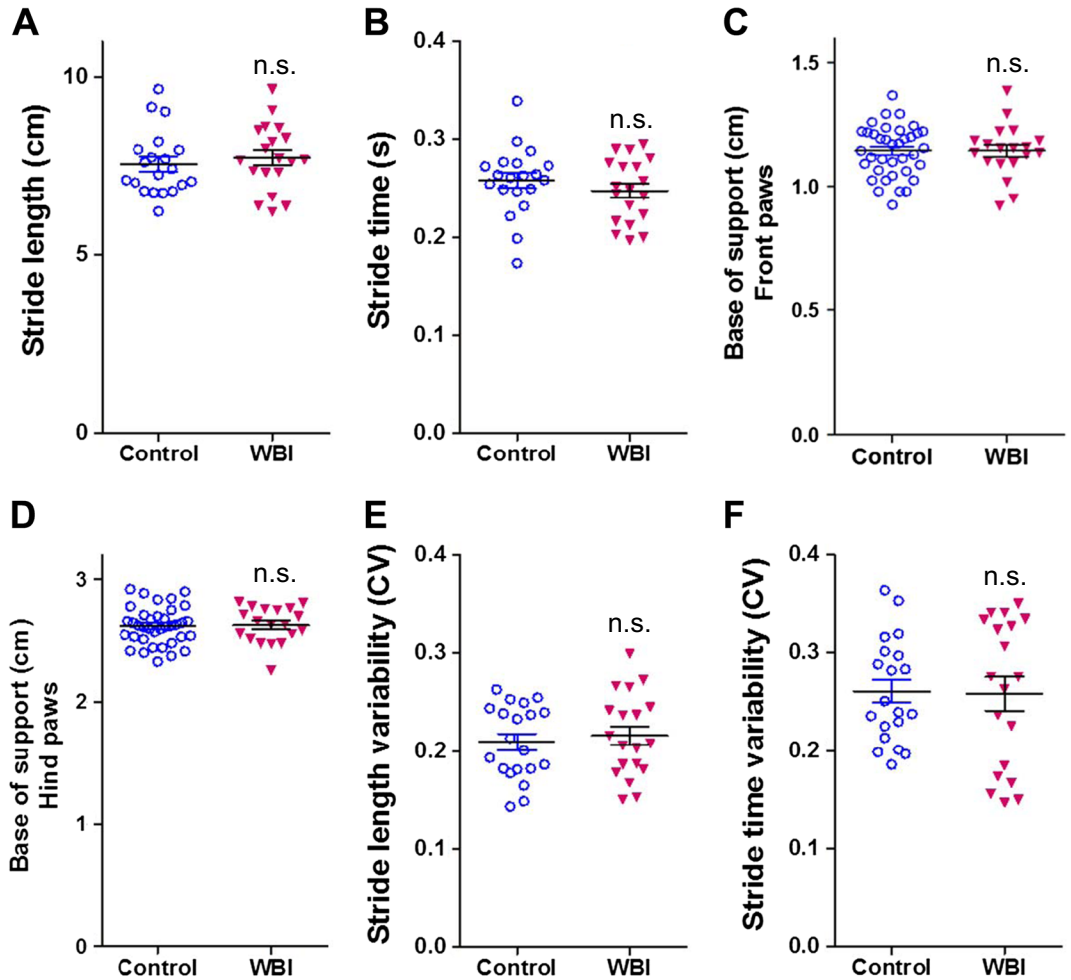

Fig. 2 Effects of WBI on gait parameters at 3 months post-treatment. Stride length (**a**), stride time (**b**), base of support (front paws); **c**), base of support (hind paws); **d**), stride length variability (**e**), and stride time variability (**f**) in control mice and WBI-treated mice at 3 months post-treatment. Data are mean ± SEM

abnormalities associated with WBI-induced accelerated brain senescence exhibit later onset than memory impairment.

Cerebromicrovascular function is significantly impaired in mice by 3 months post-WBI

In order to determine whether cerebromicrovascular dysfunction associates with cognitive decline, we assessed functional hyperemia in the whisker barrel cortex in mice at 3 months post-WBI. We found that CBF responses in the whisker barrel cortex elicited by contralateral whisker stimulation were significantly decreased in WBI-treated mice compared to control animals indicating impaired neurovascular coupling at 3 months post-irradiation (representative CBF tracings are shown in Fig. 4a, summary data are shown in Fig. 4b). WBI could reduce functional hyperemia by impairing neural activity evoked by whisker stimulation. To examine this possibility, we recorded spontaneous and evoked neural activity in control and WBI-treated mice. We found that the amplitude and frequency distribution of the electrocorticogram (data not shown) and the amplitude of the somatosensory field potentials produced by activation of the whisker pad were not different between control and WBI-treated mice (Fig. 4c). Therefore, WBI is unlikely to contribute to impaired functional hyperemia by modulating the neural activity evoked by whisker stimulation.

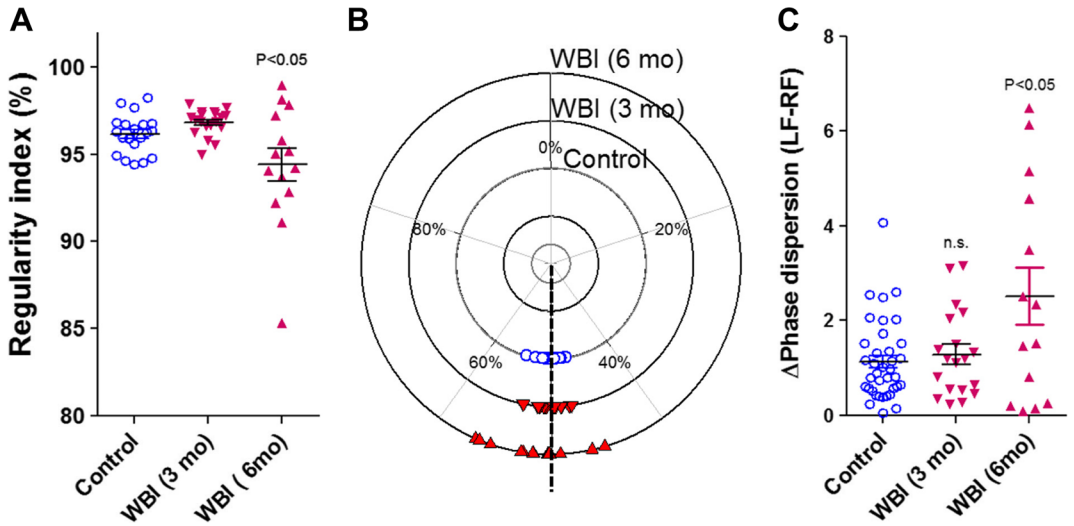

Fig. 3 WBI results in progressive gait abnormalities in mice at 6 months post-treatment. **a** Regularity index in control mice and WBI-treated mice at 3 and 6 months post-treatment. **b** Circular scatter plot showing the distribution of inter-limb coupling values (phase dispersion) in control mice and WBI-treated mice at 3 and 6 months post-treatment (note that the circular plot shows a smaller phase dispersion scatter in the inner circle (control) as compared to the phase dispersion scatter in the outer circle (assessed 6 month after WBI)). **c** This shows average deviation of phase dispersion (calculated between the right front paw (RF) and left front paw (LF)) from the expected value (50%) under baseline conditions and after WBI. Data are mean ± SEM.*$p < 0.05$ vs. control

Discussion

The key finding of his study is that in mice a clinically relevant protocol of fractionated WBI results in a significant cerebromicrovascular dysfunction, which associates with cognitive impairment, mimicking the aging phenotype.

There is growing evidence that vascular contributions to cognitive impairment and dementia (VCID) are critical in aging (Ungvari and Sonntag 2014). Among them, impaired neurovascular coupling responses (Fabiani et al. 2013; Park et al. 2007; Stefanova et al. 2013; Topcuoglu et al. 2009; Toth et al. 2014a; Zaletel et al. 2005) are thought to importantly contribute to the cognitive decline (Sorond et al. 2013) in the elderly. From the results of this study and from recent findings by other laboratories (Warrington et al. 2013), the picture emerges that WBI-induced DNA damage responses induce an accelerated aging-like phenotype in the neurovascular

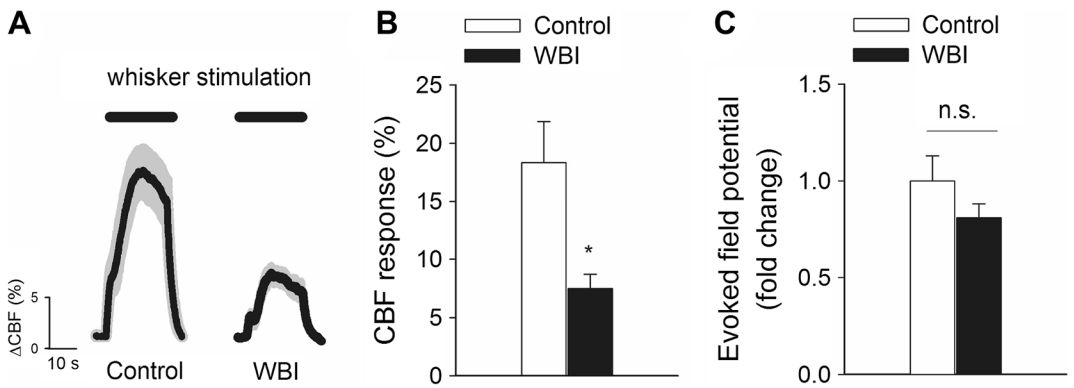

Fig. 4 Whole brain irradiation impairs neurovascular coupling responses 3 months post-WBI. **a** Representative traces of CBF measured with a laser Doppler probe above the whisker barrel cortex during contralateral whisker stimulation (5 Hz) in control and WBI-treated mice 3 months post-WBI. **b** Increases in cerebral blood flow (CBF; expressed as % of baseline) measured above the barrel field of the primary somatosensory cortex in response to whisker stimulation in control mice and in WBI-treated mice. **c** The somatosensory evoked potential responses in the somatosensory cortex evoked by contralateral whisker pad stimulation are comparable in control and WBI-treated mice. The amplitude of the negative wave of the field potentials was not significantly different. Data are mean ± S.E.M ($n = 6$, *$p < 0.05$ vs. control)

unit, which results in impaired CBF responses upon neuronal activation. We posit that impaired functional hyperemia per se may play a significant causal role in irradiation-induced cognitive impairment. Experimental studies support this concept, demonstrating that pharmacologically induced selective neurovascular uncoupling in mice mimics important aspects of both age-related and WBI-induced cognitive impairment (Tarantini et al. 2015). There are also studies extant linking impaired neurovascular coupling to gait dysfunction in the elderly (Sorond et al. 2011). Thus, we speculate that WBI-induced neurovascular coupling may also contribute to the gait/motor coordination abnormalities observed in our present study as well as in previous reports (Brown et al. 2016; Hatcher-Martin and Factor 2016). Further studies are warranted to determine whether changes in gait after WBI correlate with the severity of post-radiation cerebromicrovascular deficits. Previous studies by us and others have shown that WBI also results in a significant microvascular rarefaction (Ljubimova et al. 1991; Warrington et al. 2012), particularly in the hippocampus, the region responsible for spatial learning and memory (Warrington et al. 2011). It is likely that neurovascular uncoupling and microvascular rarefaction act synergistically to impair regional blood supply in the brain (Fuss et al. 2000; Taki et al. 2002), exacerbating cognitive decline. It is important that both neurovascular dysfunction and microvascular rarefaction are manifested relatively early (within 3 months) after WBI and their onset coincides with the appearance of cognitive symptoms.

The mechanisms underlying WBI-induced neurovascular dysfunction are presently unknown and should be elucidated in future studies. Neurovascular coupling depends on an intact functional network of neurons, astrocytes, and vascular cells (Attwell et al. 2010; Chen et al. 2014). Unlike neurons, cells of the neurovascular unit (including astrocytes and endothelial cells) are radiosensitive (Ungvari et al. 2013). There is evidence that WBI significantly impacts astrocytes, the functional impairment of which has also been linked to radiation-induced blood brain barrier disruption (Gaber et al. 2004; Yuan et al. 2006; Yuan et al. 2003; Yuan et al. 2005). The astrocytic mechanisms underlying neurovascular coupling include production and release of vasodilator metabolites of arachidonic acid, including epoxygenase-derived epoxyeicosatrienoic acids (EETs) and cyclooxygenase-derived prostaglandins (Peng et al. 2002; Takano et al. 2006; Zonta et al. 2003). Future studies should determine how DNA damage responses in astrocytes alter the synthesis/release of these mediators. There is also strong experimental evidence that endothelial NO production contributes to glio-vascular coupling (Chen et al. 2014; Girouard et al. 2007; Longden and Nelson 2011; Ma et al. 1996; Stobart et al. 2013; Toth et al. 2015b). Because the phenotype of cerebromicrovascular endothelial cells can also be altered by irradiation-induced DNA damage (Ungvari et al. 2013; Warrington et al. 2013); future studies should also determine the role of endothelial dysfunction in WBI-induced impairment of functional hyperemia.

In conclusion, our results add to the growing evidence that stressors that cause DNA damage promote the development of complex aging-like phenotypic changes in the brain, which are characterized by functional and structural impairment of the cerebral microcirculation. It is significant that cognitive decline due to microvascular causes is potentially reversible (Warrington et al. 2011, 2012). Our findings, taken together with the results of earlier studies (reviewed in Warrington et al. (2013)), point to potential benefits of interventions that rescue glio-vascular coupling mechanisms and promote microvascular health for prevention of cognitive decline both in WBI-treated patients and the elderly. There is increasing realization that DNA damage-induced cellular senescence programs play a critical role in brain aging process (reviewed in Chinta et al. (2014)), thus we propose that the present clinically relevant model of fractionated WBI should be considered to study fundamental mechanisms of brain and cognitive aging as well.

Acknowledgements This work was supported by grants from the Reynolds Foundation (to AY), the American Heart Association (to ST, AC and ZU), the National Center for Complementary and Alternative Medicine (R01-AT006526), the National Institute on Aging (R01-AG047879; R01-AG038747; 3P30AG050911-02S1), the National Institute of Neurological Disorders and Stroke (NINDS; R01-NS056218), the Oklahoma Center for the Advancement of Science and Technology (to AY, AC, ZU) and the IBEST-OUHSC (to AY).

Compliance with ethical standards

Disclosure None.

References

Ashpole NM, Warrington JP, Mitschelen MC, Yan H, Sosnowska D, Gautam T, Farley JA, Csiszar A, Ungvari Z, Sonntag WE

(2014) Systemic influences contribute to prolonged microvascular rarefaction after brain irradiation: a role for endothelial progenitor cells. Am J Physiol Heart Circ Physiol 307: H858–H868

Attwell D, Buchan AM, Charpak S, Lauritzen M, Macvicar BA, Newman EA (2010) Glial and neuronal control of brain blood flow. Nature 468:232–243

Brown PD, Jaeckle K, Ballman KV, Farace E, Cerhan JH, Anderson SK, Carrero XW, Barker FG 2nd, Deming R, Burri SH, Menard C, Chung C, Stieber VW, Pollock BE, Galanis E, Buckner JC, Asher AL (2016) Effect of radiosurgery alone vs radiosurgery with whole brain radiation therapy on cognitive function in patients with 1 to 3 brain metastases: a randomized clinical trial. JAMA 316:401–409

Chen BR, Kozberg MG, Bouchard MB, Shaik MA, Hillman EM (2014) A critical role for the vascular endothelium in functional neurovascular coupling in the brain. J Am Heart Assoc 3:e000787

Chinta SJ, Woods G, Rane A, Demaria M, Campisi J, and Andersen JK 2014 Cellular senescence and the aging brain. Exp Gerontol

Fabiani M, Gordon BA, Maclin EL, Pearson MA, Brumback-Peltz CR, Low KA, McAuley E, Sutton BP, Kramer AF, and Gratton G 2013 Neurovascular coupling in normal aging: A combined optical, ERP and fMRI study. Neuroimage

Fuss M, Wenz F, Scholdei R, Essig M, Debus J, Knopp MV, Wannenmacher M (2000) Radiation-induced regional cerebral blood volume (rCBV) changes in normal brain and low-grade astrocytomas: quantification and time and dose-dependent occurrence. Int J Radiat Oncol Biol Phys 48:53–58

Gaber MW, Yuan H, Killmar JT, Naimark MD, Kiani MF, Merchant TE (2004) An intravital microscopy study of radiation-induced changes in permeability and leukocyte-endothelial cell interactions in the microvessels of the rat pia mater and cremaster muscle. Brain Res Brain Res Protoc 13:1–10

Gaspar LE, Mehta MP, Patchell RA, Burri SH, Robinson PD, Morris RE, Ammirati M, Andrews DW, Asher AL, Cobbs CS, Kondziolka D, Linskey ME, Loeffler JS, McDermott M, Mikkelsen T, Olson JJ, Paleologos NA, Ryken TC, Kalkanis SN (2010) The role of whole brain radiation therapy in the management of newly diagnosed brain metastases: a systematic review and evidence-based clinical practice guideline. J Neuro-Oncol 96:17–32

Girouard H, Park L, Anrather J, Zhou P, Iadecola C (2007) Cerebrovascular nitrosative stress mediates neurovascular and endothelial dysfunction induced by angiotensin II. Arterioscler Thromb Vasc Biol 27:303–309

Hatcher-Martin JM, Factor SA (2016) Freezing of gait: a rare delayed complication of whole brain radiation. Parkinsonism Relat Disord 29:129–130

Khuntia D, Brown P, Li J, Mehta MP (2006) Whole-brain radiotherapy in the management of brain metastasis. J Clin Oncol 24:1295–1304

Lamproglou I, Martin S, Diserbo M, Multon E, Petiet A, Colas-Linhart N, Bok B, Martin C (2001) Total body 4.5 Gy gamma irradiation-induced early delayed learning and memory dysfunction in the rat. Cell Mol Biol (Noisy-le-grand) 47:453–457

Lee YW, Cho HJ, Lee WH, Sonntag WE (2012) Whole brain radiation-induced cognitive impairment: pathophysiological mechanisms and therapeutic targets. Biomol Ther (Seoul) 20: 357–370

Ljubimova NV, Levitman MK, Plotnikova ED, Eidus L (1991) Endothelial cell population dynamics in rat brain after local irradiation. Br J Radiol 64:934–940

Longden T and Nelson M. Recruitment of the Vascular Endothelium into Neurovascular Coupling. *Proceedings of the British Pharmacological Society at* http://wwwpA2onlineorg/abstracts/Vol9Issue3abst062Ppdf 9: 062P, 2011

Ma J, Ayata C, Huang PL, Fishman MC, Moskowitz MA (1996) Regional cerebral blood flow response to vibrissal stimulation in mice lacking type I NOS gene expression. Am J Phys 270:H1085–H1090

Park L, Anrather J, Girouard H, Zhou P, Iadecola C (2007) Nox2-derived reactive oxygen species mediate neurovascular dysregulation in the aging mouse brain. J Cereb Blood Flow Metab 27:1908–1918

Patil CG, Pricola K, Sarmiento JM, Garg SK, Bryant A, Black KL (2012) Whole brain radiation therapy (WBRT) alone versus WBRT and radiosurgery for the treatment of brain metastases. Cochrane Database Syst Rev 9:CD006121

Peng X, Carhuapoma JR, Bhardwaj A, Alkayed NJ, Falck JR, Harder DR, Traystman RJ, Koehler RC (2002) Suppression of cortical functional hyperemia to vibrissal stimulation in the rat by epoxygenase inhibitors. Am J Physiol Heart Circ Physiol 283:H2029–H2037

Shi L, Adams MM, Long A, Carter CC, Bennett C, Sonntag WE, Nicolle MM, Robbins M, D'Agostino R, Brunso-Bechtold JK (2006) Spatial learning and memory deficits after whole-brain irradiation are associated with changes in NMDA receptor subunits in the hippocampus. Radiat Res 166:892–899

Sorond FA, Kiely DK, Galica A, Moscufo N, Serrador JM, Iloputaife I, Egorova S, Dell'Oglio E, Meier DS, Newton E, Milberg WP, Guttmann CR, Lipsitz LA (2011) Neurovascular coupling is impaired in slow walkers: the MOBILIZE Boston study. Ann Neurol 70:213–220

Sorond FA, Hurwitz S, Salat DH, Greve DN, and Fisher ND. Neurovascular coupling, cerebral white matter integrity, and response to cocoa in older people. Neurology, 2013.

Soussain C, Ricard D, Fike JR, Mazeron JJ, Psimaras D, Delattre JY (2009) CNS complications of radiotherapy and chemotherapy. Lancet 374:1639–1651

Stefanova I, Stephan T, Becker-Bense S, Dera T, Brandt T, Dieterich M (2013) Age-related changes of blood-oxygen-level-dependent signal dynamics during optokinetic stimulation. Neurobiol Aging 34:2277–2286

Stobart JL, Lu L, Anderson HD, Mori H, Anderson CM (2013) Astrocyte-induced cortical vasodilation is mediated by D-serine and endothelial nitric oxide synthase. Proc Natl Acad Sci U S A 110:3149–3154

Takano T, Tian GF, Peng W, Lou N, Libionka W, Han X, Nedergaard M (2006) Astrocyte-mediated control of cerebral blood flow. Nat Neurosci 9:260–267

Taki S, Higashi K, Oguchi M, Tamamura H, Tsuji S, Ohta K, Tonami H, Yamamoto I, Okamoto K, Iizuka H (2002) Changes in regional cerebral blood flow in irradiated regions and normal brain after stereotactic radiosurgery. Ann Nucl Med 16:273–277

Tarantini S, Hertelendy P, Tucsek Z, Valcarcel-Ares MN, Smith N, Menyhart A, Farkas E, Hodges EL, Towner R, Deak F, Sonntag WE, Csiszar A, Ungvari Z, Toth P (2015) Pharmacologically-induced neurovascular uncoupling is associated with cognitive impairment in mice. J Cereb Blood Flow Metab 35:1871–1881

Tarantini S, Tran CH, Gordon GR, Ungvari Z, Csiszar A (2016) Impaired neurovascular coupling in aging and Alzheimer's disease: contribution of astrocyte dysfunction and endothelial impairment to cognitive decline. Exp Gerontol. doi:10.1016/j.exger.2016.1011.1004

Topcuoglu MA, Aydin H, Saka E (2009) Occipital cortex activation studied with simultaneous recordings of functional transcranial Doppler ultrasound (fTCD) and visual evoked potential (VEP) in cognitively normal human subjects: effect of healthy aging. Neurosci Lett 452:17–22

Toth P, Tarantini S, Tucsek Z, Ashpole NM, Sosnowska D, Gautam T, Ballabh P, Koller A, Sonntag WE, Csiszar A, Ungvari ZI (2014a) Resveratrol treatment rescues neurovascular coupling in aged mice: role of improved cerebromicrovascular endothelial function and down-regulation of NADPH oxidase. Am J Physiol Heart Circ Physiol 306:H299–H308

Toth P, Tucsek Z, Tarantini S, Sosnowska D, Gautam T, Mitschelen M, Koller A, Sonntag WE, Csiszar A, Ungvari Z (2014b) IGF-1 deficiency impairs cerebral myogenic autoregulation in hypertensive mice. J Cereb Blood Flow Metab 34:1887–1897

Toth P, Tarantini S, Ashpole NM, Tucsek Z, Milne GL, Valcarcel-Ares NM, Menyhart A, Farkas E, Sonntag WE, Csiszar A, Ungvari Z (2015a) IGF-1 deficiency impairs neurovascular coupling in mice: implications for cerebromicrovascular aging. Aging Cell 14:1034–1044

Toth P, Tarantini S, Davila A, Valcarcel-Ares MN, Tucsek Z, Varamini B, Ballabh P, Sonntag WE, Baur JA, Csiszar A, Ungvari Z (2015b) Purinergic glio-endothelial coupling during neuronal activity: role of P2Y1 receptors and eNOS in functional hyperemia in the mouse somatosensory cortex. Am J Physiol Heart Circ Physiol 309:H1837–H1845

Toth P, Szarka N, Farkas E, Ezer E, Czeiter E, Amrein K, Ungvari Z, Hartings JA, Buki A, Koller A (2016) Traumatic brain injury-induced autoregulatory dysfunction and spreading depression-related neurovascular uncoupling: Pathomechanisms, perspectives, and therapeutic implications. Am J Physiol Heart Circ Physiol 311:H1118–H1131

Toth P, Tarantini S, Csiszar A, Ungvari Z (2017) Functional vascular contributions to cognitive impairment and dementia: mechanisms and consequences of cerebral autoregulatory dysfunction, endothelial impairment, and neurovascular uncoupling in aging. Am J Physiol Heart Circ Physiol 312:H1–H20

Tucsek Z, Toth P, Tarantini S, Sosnowska D, Gautam T, Warrington JP, Giles CB, Wren JD, Koller A, Ballabh P, Sonntag WE, Ungvari Z, Csiszar A (2014) Aging exacerbates obesity-induced cerebromicrovascular rarefaction, neurovascular uncoupling, and cognitive decline in mice. J Gerontol A Biol Sci Med Sci 69:1339–1352

Ungvari Z, Sonntag WE (2014) Brain and cerebrovascular aging—new mechanisms and insights. J Gerontol A Biol Sci Med Sci 69:1307–1310

Ungvari Z, Podlutsky A, Sosnowska D, Tucsek Z, Toth P, Deak F, Gautam T, Csiszar A, Sonntag WE (2013) Ionizing radiation promotes the acquisition of a senescence-associated secretory phenotype and impairs angiogenic capacity in cerebromicrovascular endothelial cells: role of increased DNA damage and decreased DNA repair capacity in microvascular radiosensitivity. J Gerontol A Biol Sci Med Sci 68:1443–1457

Warrington JP, Csiszar A, Johnson DA, Herman TS, Ahmad S, Lee YW, Sonntag WE (2011) Cerebral microvascular rarefaction induced by whole brain radiation is reversible by systemic hypoxia in mice. Am J Physiol Heart Circ Physiol 300:H736–H744

Warrington JP, Csiszar A, Mitschelen M, Lee YW, Sonntag WE (2012) Whole brain radiation-induced impairments in learning and memory are time-sensitive and reversible by systemic hypoxia. PLoS One 7:e30444

Warrington JP, Ashpole N, Csiszar A, Lee YW, Ungvari Z, Sonntag WE (2013) Whole brain radiation-induced vascular cognitive impairment: mechanisms and implications. J Vasc Res 50:445–457

Welzel G, Fleckenstein K, Mai SK, Hermann B, Kraus-Tiefenbacher U, Wenz F (2008a) Acute neurocognitive impairment during cranial radiation therapy in patients with intracranial tumors. Strahlenther Onkol 184:647–654

Welzel G, Fleckenstein K, Schaefer J, Hermann B, Kraus-Tiefenbacher U, Mai SK, Wenz F (2008b) Memory function before and after whole brain radiotherapy in patients with and without brain metastases. Int J Radiat Oncol Biol Phys 72:1311–1318

Yuan H, Gaber MW, McColgan T, Naimark MD, Kiani MF, Merchant TE (2003) Radiation-induced permeability and leukocyte adhesion in the rat blood-brain barrier: modulation with anti-ICAM-1 antibodies. Brain Res 969:59–69

Yuan H, Goetz DJ, Gaber MW, Issekutz AC, Merchant TE, Kiani MF (2005) Radiation-induced up-regulation of adhesion molecules in brain microvasculature and their modulation by dexamethasone. Radiat Res 163:544–551

Yuan H, Gaber MW, Boyd K, Wilson CM, Kiani MF, Merchant TE (2006) Effects of fractionated radiation on the brain vasculature in a murine model: blood-brain barrier permeability, astrocyte proliferation, and ultrastructural changes. Int J Radiat Oncol Biol Phys 66:860–866

Zaletel M, Strucl M, Pretnar-Oblak J, Zvan B (2005) Age-related changes in the relationship between visual evoked potentials and visually evoked cerebral blood flow velocity response. Funct Neurol 20:115–120

Zonta M, Angulo MC, Gobbo S, Rosengarten B, Hossmann KA, Pozzan T, Carmignoto G (2003) Neuron-to-astrocyte signaling is central to the dynamic control of brain microcirculation. Nat Neurosci 6:43–50